

Aharonov-Bohm effect in quasi-one-dimensional $\text{In}_{0.77}\text{Ga}_{0.23}\text{As}/\text{InP}$ rings

J. Appenzeller, Th. Schäpers, H. Hardtdegen, B. Lengeler, and H. Lüth
*Institut für Schicht- und Ionentechnik, Forschungszentrum Jülich G.m.b.H.,
 52425 Jülich, Germany*
 (Received 22 September 1994)

Aharonov-Bohm oscillations with a modulation of the resistance amplitude up to 12% have been observed in high mobility $\text{In}_x\text{Ga}_{1-x}\text{As}/\text{InP}$ rings. The phase coherence length L_Φ is extracted from the interference pattern by an analysis of the oscillation amplitude as a function of temperature and electron excess energy. L_Φ shows approximately a $T^{-0.5}$ dependence for temperatures between 2 and 10 K. We attribute this behavior to momentum-nonconserving processes in a quasi-one-dimensional ring structure. Although the widths of the samples are comparable to the Fermi wavelength there is still more than one one-dimensional conducting channel in the ring and the phase coherence length saturates for decreasing temperature.

I. INTRODUCTION

In future quantum electronics the interference of an electron on different Feynman trajectories might become relevant for device applications. Aharonov-Bohm type experiments are of central interest for studying the underlying phenomena and for testing the suitability of possible semiconductor structures. The relevant length scale for interference phenomena is the phase coherence length L_Φ . Inelastic scattering of the electrons at phonons is one source of coherency destroying events. Another is electron-electron scattering of hot electrons, as was shown experimentally in a Young double slit experiment by Laikhtman *et al.*¹ and by us for the ballistic transport of hot electrons propagating in a two-dimensional electron gas (2DEG) between two point contacts.² Störmer *et al.*³ have shown that the acoustic phonon scattering rate decreases as T^5 at low temperatures in a two-dimensional electron gas. In quasi-one-dimensional structures, it is expected to be reduced still further due to the smaller phase space available for electron-phonon scattering events. In two dimensions, average times as long as 10^{-9} s between scattering events than the expected time when electron-electron interaction dominates the scattering.

Theoretical investigations of the effect of electron-electron scattering in one-dimensional geometries were performed by Fasol.⁴ His simulations showed, that τ_{ee} does not saturate in an ideal single mode quantum wire at low temperatures. Only the well known temperature dependence of τ_{ee} limits the phase coherence length. In this regime, Fasol predicted an enhancement of L_Φ up to a few mm at mK temperatures. In two dimensions, on the other hand a second contribution to electron-electron scattering limits τ_{ee} . Current flows only when a certain fraction of carriers have an excess energy relative to the Fermi level. This excess energy gives rise to electron-electron scattering which is temperature independent and which ultimately limits τ_{ee} . In one dimension a reduction in phase space strongly suppresses this second contribu-

tion.

In the present study, we have investigated rings of small width in the strained $\text{In}_{0.77}\text{Ga}_{0.23}\text{As}/\text{InP}$ system in order to determine the inelastic mean free path as a function of temperature. An increase of temperature leads to an enhanced probability of electron-electron scattering events, thus reducing the phase coherence length. Measuring the amplitude of the Aharonov-Bohm oscillations versus temperature is a precise method for the analysis of $L_\Phi(T)$.⁵ As is shown in the present paper, the $\text{In}_x\text{Ga}_{1-x}\text{As}/\text{InP}$ system is ideally suited for this application due to the very small effective mass of the electrons in the two-dimensional sheet and due to the high electron concentration and electron mobility, which can be achieved without occupation of a second subband. In addition, there is no depletion zone at the edges of the rings when structuring is done by reactive ion etching, so that the lithographical and the conducting widths are identical.

We have observed Aharonov-Bohm oscillations with an amplitude about 10% of the device resistance. Even at 10 K the Fourier spectrum of the data shows a pronounced feature, which is clearly identified as the h/e peak. Furthermore, we report on the temperature dependence of L_Φ for a number of different electron excess energies.

II. DEVICE FABRICATION

Modulation doped $\text{In}_{0.77}\text{Ga}_{0.23}\text{As}/\text{InP}$ heterostructures with a 2DEG in the ternary compound were used in the present investigation. The structures were grown by low pressure metal organic vapor phase epitaxy. They consist of a 10 nm thick *n*-doped spike of InP ($N_D = 4.2 \times 10^{17} \text{ cm}^{-3}$) followed by a 20 nm InP spacer layer and a 10 nm thick $\text{In}_{0.77}\text{Ga}_{0.23}\text{As}$ channel, which is finally capped with a 150 nm thick $\text{In}_{0.53}\text{Ga}_{0.47}\text{As}$ top layer.^{6,7} Due to the high In content the channel layer is highly strained.

The Aharonov-Bohm rings were fabricated using electron beam lithography and reactive ion etching (RIE). A 30 nm thick layer of SiO₂ was deposited on the surface of the system followed by electron sensitive resist polymethyl methacrylate (PMMA). Using the resist after electron beam lithography to transcribe the relevant pattern to the SiO₂ by a CHF₃ RIE process, the oxide serves as a mask for the semiconductor and ensures smooth edges of the sample. Otherwise, if PMMA itself is used as a mask during the etching, the resist is heated up and the edges become very rough. We have applied a H₂/CH₄ plasma with etch rates of 15 nm/min in InP and 9 nm/min in In_xGa_{1-x}As.

The RIE process removes the In_xGa_{1-x}As layers and thereby destroys the 2DEG which leads to electron confinement in the nonetched area. By means of this technique, we have defined Aharonov-Bohm rings with a width (W) of about 85 nm. The average diameter of the rings is $2r = 0.7 \mu\text{m}$. The Ohmic contacts consist of alloyed Ni/AuGe/Ni (5 nm/90 nm/25 nm) packages. Cr/Au (5 nm/100 nm) bond pads were deposited on top of the probes. Figure 1 shows a scanning electron micrograph of the ring.

The electron density (n_s) and mobility (μ) at 4.2 K determined by Hall effect are $n_s \approx 5.9 \times 10^{11} \text{ cm}^{-2}$ and $\mu \approx 37 \text{ m}^2/\text{Vs}$, respectively. Thus, the Fermi wavelength is $\lambda_F \approx 33 \text{ nm}$ and the elastic mean free path $L_{el} \approx 4.7 \mu\text{m}$. This distance cannot be interpreted as the average distance between impurities L_{bal} . Small angle scattering events like scattering at ionized impurities are not detected directly in the Hall effect. Fits to SdH oscillations in the low field regime⁸ yield a ballistic mean free path around five times smaller.

The mobility of our devices is excellent in view of the fact that the 2DEG is located in the ternary compound, where alloy disorder adds to the scattering of the carriers. With these parameters, we are in a regime where $\lambda_F \sim W$, $W \ll L_{bal}, L_{\Phi}$ and $2\pi r \sim L_{bal}, L_{\Phi}$ (as will be shown later). Compared to the experiments performed by Webb and Washburn⁹⁻¹¹ on metallic samples, we achieve oscillation values $\Delta R/R$ about 100 times larger in amplitude. This is due to the fact that $\lambda_F \sim W$ in 2DEG's at semiconductor heterointerfaces, in contrast to metals, where a large number of conducting channels exists at the Fermi energy.

III. RESULTS AND DISCUSSION

All our samples were measured in a four-terminal configuration using standard lock-in techniques. To reach temperatures down to 330 mK we used a ³He-evaporation cryostat with a superconducting magnet.

In Fig. 2(a) the magnetoresistance (R_{xx}) versus magnetic field (B) is plotted at $T = 330 \text{ mK}$ for a current of 1 nA through the ring. Very clear oscillations with an amplitude of up to 1 k Ω on a background resistance of around 8.5 k Ω are resolved. To estimate the widths of the rings, we have assumed the limits of the h/e peak in the Fourier transform [Fig. 2(b)] to be directly related to the minimum and maximum enclosed area of the annulus. This leads to an inner diameter of 648 nm and an outer one of 819 nm, in excellent agreement with the lithographical data.

Besides the h/e peak, a second structure can be seen in Fig. 2(b) corresponding to an oscillation with a fre-

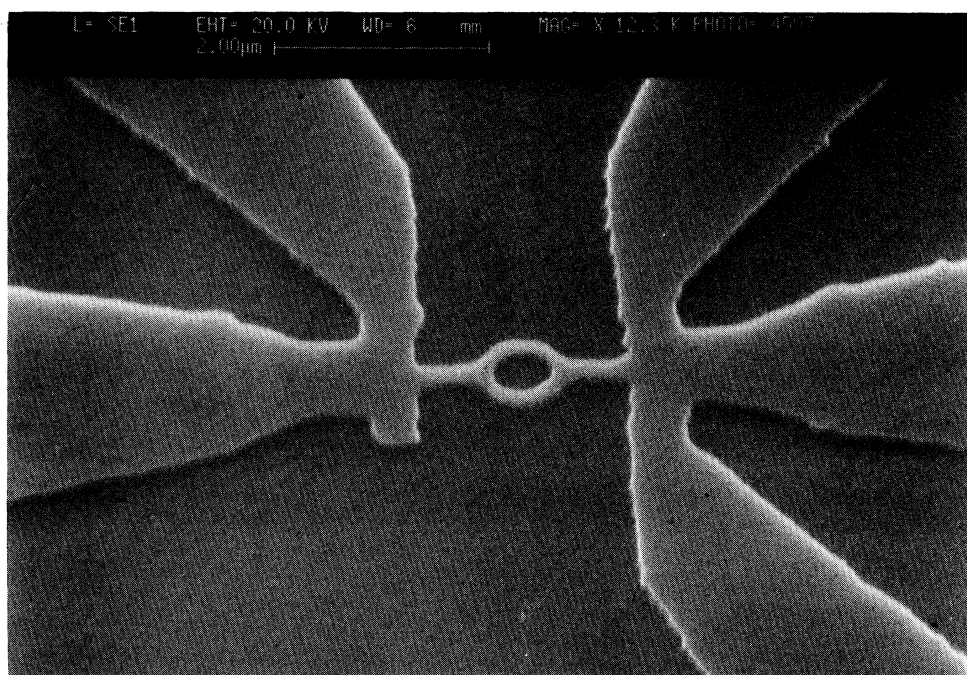


FIG. 1. Scanning electron micrograph of a typical ring under investigation.

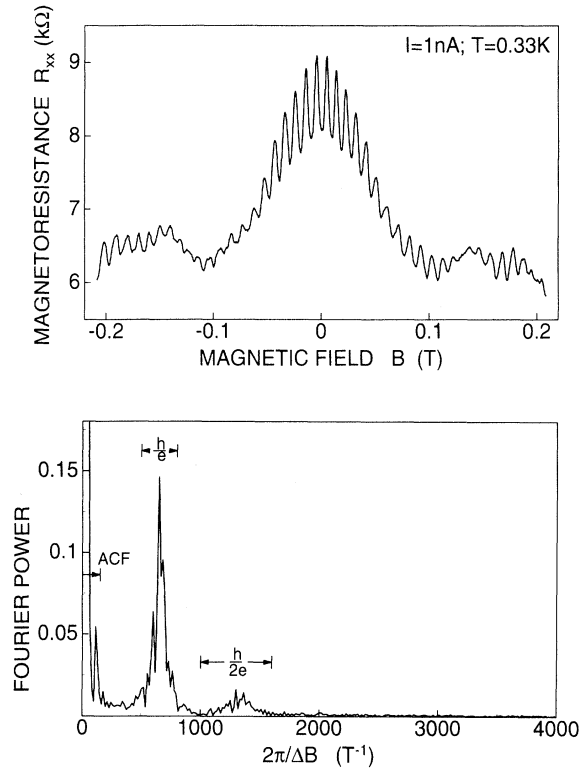


FIG. 2. (a) Magnetoresistance of $\text{In}_{0.77}\text{Ga}_{0.23}\text{As}/\text{InP}$ quantum wire ring versus magnetic field normal to the ring at $T = 0.33$ K and a current $I = 1$ nA. (b) Fourier power spectrum of the data from Fig. 2(a). Peaks corresponding to h/e and $h/2e$ oscillations are found. The harmonic $h/2e$ is indicative of electron trajectories which encircle the annulus twice.

quency of $h/2e$. There are two possible explanations for such a peak: weak localization and second harmonic Aharonov-Bohm oscillations. Al'tshuler, Aronov, Spivak oscillations⁹ due to weak localization are well known to appear in doubly connected geometries but are suppressed already for magnetic fields of a few mT. Since the field range for the observed oscillations exceeds by far this value, we conclude that the period $h/2e$ is due to second harmonic Aharonov-Bohm oscillations, i.e., due to trajectories which encircle twice the annulus.¹² The Fourier periods of the h/e and $h/2e$ oscillations were independent of temperature in the range investigated.

The oscillations are superimposed upon a magnetoresistance peak around $B = 0$. This peak arises from quantum mechanical and classical corrections to the classical Drude conductivity in the quasiballistic regime.¹³ Figure 3 shows the magnetoresistance background and its magnetic field dependence up to the onset of Shubnikov-de Haas (SdH) oscillations at $B \approx 1.5$ T for a sample similar to that in Figs. 2(a) and 2(b). For a wire width W smaller than L_{bal} the influence of the boundaries produces a parabolic negative magnetoresistance. In addition, weak localization reduces the conductivity for small magnetic fields (for a detailed discussion see Ref. 13). Furthermore, aperiodic conductance fluctuations due to

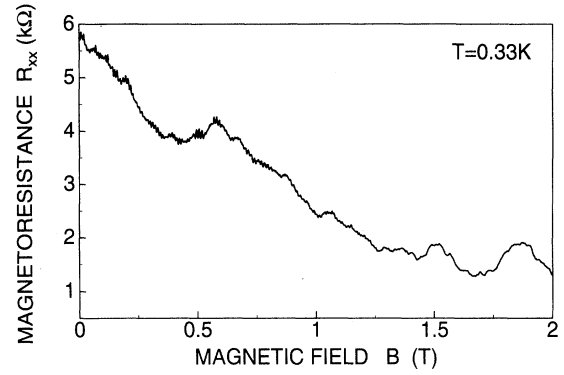


FIG. 3. Magnetoresistance R_{xx} for a field scan up to $B = 2$ T. Aharonov-Bohm oscillations are superimposed upon a resistance peak around $B = 0$ arising from classical and quantum mechanical corrections due to the one-dimensional transport properties.

quantum interference of randomly scattered electrons are visible in Fourier transform at $2\pi/\Delta B \approx 0$, indicating that the pure ballistic limit is still not reached.

We first consider these aperiodic conductance fluctuations (ACF). The average amplitude ΔG_{CF} of the ACF can be used to determine the phase coherence length. At $T = 0$ the amplitude of these fluctuations is of the order of e^2/h , independent of sample size or degree of disorder.¹⁴ At finite temperature this situation is altered and ΔG_{CF} depends on the channel length. When the thermal diffusion length L_T (the distance an electron can diffuse before the uncertainty in its energy becomes less than $k_B T$) is larger than the sample size, the amplitude of conductance fluctuations is given by an expression independent of L_T (Ref. 15),

$$\Delta G_{\text{CF}} = \frac{\Delta R}{R^2} = \frac{e^2}{h} \left(\frac{L_\Phi}{L_{\text{tot}}} \right)^{\frac{3}{2}}, \quad (1)$$

where $L_{\text{tot}} \approx 2.75 \mu\text{m}$ is the total voltage probe separation in the samples. Using this value in Eq. (1), the phase coherence length for a current of 1 nA and a temperature of 330 mK turns out to be $(1.1 \pm 0.12) \mu\text{m}$.

We now consider the Aharonov-Bohm oscillations. The Aharonov-Bohm oscillations in Fig. 3 show a decreasing amplitude for increasing magnetic field and vanish for $B \approx 1.2$ T. Timp *et al.*¹² have discussed a very similar suppression of the Aharonov-Bohm effect with increasing magnetic field in $\text{GaAs}/\text{Al}_x\text{Ga}_{1-x}\text{As}$ rings. They agree with the proposition of Datta and Bandyopadhyay¹⁶ that the wave function may be localized within one branch of the annulus if the Larmor radius becomes equal to half the wire width, then suppressing the quantum interference. In our case, the critical field is determined as 0.4 T for $W = 85$ nm and, thus, in the following, we restrict ourselves to the analysis of the periodic oscillations for $B < 0.4$ T. In this magnetic field range no monotonous decay of oscillation amplitude with magnetic field is apparent and, therefore, we have not included any asymmetry in the splitting of the electron wave function in the

annulus.

A detailed theory of the quantum transport properties in a ring is not yet available. Nevertheless, we will now give an expression for the Aharonov-Bohm amplitudes which, we believe, contains the major dependences on the characteristic lengths. As outlined above, the ballistic mean free path L_{bal} deduced from SdH oscillations has a value of $0.9 \mu\text{m}$ as compared to a separation of the voltage probes by $2.75 \mu\text{m}$. So, we are in the diffusive transport regime which is characterized by an exponential decay of the amplitude as a function of distance. For the Aharonov-Bohm oscillations, the relevant distance is the circumference, $2\pi r$, of the ring. Thus, we assume the amplitude to be proportional $\exp[-2\pi r/L_\Phi]$.

Besides this effect of L_Φ on the conductance variation ΔG_{AB} , often an additional term can be found which includes the influence of thermal energy averaging.¹¹ Two Feynman trajectories for a diffusing electron, traversed with an energy difference $k_B T$, are out of phase when the distance traveled becomes larger than the thermal length $L_T = \sqrt{\hbar D/k_B T}$, where D is the diffusion constant of the carriers. The reduction of ΔG_{AB} for increasing temperature is included by a factor $\pi L_T/L_{\text{tot}}$ for $\pi L_T < L_{\text{tot}}$ and 1 for $\pi L_T > L_{\text{tot}}$. The question now arises which value to use for the diffusion constant D . In a wire in which the electrons suffer only specular boundary scattering and hence electron momentum along the wire is conserved, D takes the value of the two-dimensional electron gas. Van Houten *et al.*¹³ have discussed the change of D if diffuse boundary scattering becomes dominant in a wire. There are three reasons why in our case predominantly specular scattering is assumed in the following discussion. First, diffuse scattering leads to a reduced diffusion constant and is expected to manifest itself in a positive magnetoresistance around $B = 0$,¹⁷ which was not observed in our measurements. Second, focusing experiments with point contacts using the same heterostructure with very similar etching parameters clearly demonstrate a specularly coefficient larger than 0.7.¹⁸ Finally, using $D = (v_F W/\pi) \ln[L_{\text{el}}/W]$ for diffuse boundary scattering¹³ would yield an unreasonable maximum of L_Φ around $T = 1$ K since the measured values of ΔG_{AB} are nearly constant below $T = 2$ K, whereas $\pi L_T/L_{\text{tot}}$ with D from above would yield $\pi L_T/L_{\text{tot}} < 1$ already for $T > 0.65$ K. The expected dependence of L_Φ on temperature is discussed below. There is no reason for an increase of phase coherence length with increasing temperature. Although we cannot really exclude a small influence of electrons being scattered diffusely at the boundaries, we have used the two-dimensional value of D for calculating the thermal length L_T . For instance, for the highest temperature used in this investigation ($T = 10$ K), πL_T turns out to be $3.26 \mu\text{m}$. For lower temperatures πL_T is even larger. So, we are always in the regime where $\pi L_T/L_{\text{tot}}$ has to be replaced by 1.

Thus, the Aharonov-Bohm amplitude reads,

$$\Delta G_{\frac{h}{2e}} = \mathcal{A} \frac{e^2}{h} \exp\left[-\frac{2\pi r}{L_\Phi}\right]. \quad (2)$$

\mathcal{A} is a factor which we do not know. We determine its

value under the assumption that it is independent of temperature T and of excitation energy Δ of monoenergetic electrons relative to E_F . Fitting the data of Fig. 2(a) with Eq. (2) with $r = 0.376 \mu\text{m}$ [deduced from the Fourier peak maximum in Fig. 2(b)] and $L_\Phi = 1.1 \mu\text{m}$ (taken from the conductance fluctuations) gives $\mathcal{A} = 2.21$. We now check the consistency of the analysis by evaluating the second harmonic contribution in Fig. 2(b). An expression similar to $\Delta G_{\frac{h}{2e}}$ can be derived for $\Delta G_{\frac{h}{2e}}$:

$$\Delta G_{\frac{h}{2e}} = \mathcal{B} \frac{e^2}{h} \exp\left[-\frac{4\pi r}{L_\Phi}\right]. \quad (3)$$

Note the length $4\pi r$ for the Feynman trajectories encircling the annulus twice. Analyzing the data from Figs. 2(a), 2(b) with Eq. (3) gives a value of \mathcal{B} equal to \mathcal{A} , within the error bars of L_Φ . This is a reasonable result. Indeed, the finite width of the ring implies Fourier peaks in the Aharonov-Bohm spectrum of finite width, with a broadening increasing with the harmonic number. In other words, \mathcal{B} should not exceed \mathcal{A} . This is what we observe within the error bar. Hence, our model for the Aharonov-Bohm amplitudes leading to Eqs. (2) and (3) is apparently based on reasonable assumptions.

We now consider the influence of temperature and current on the Aharonov-Bohm amplitudes. Having determined \mathcal{A} , we will analyze our data by means of Eq. (2) and determine $L_\Phi(T, \Delta)$. Δ , the electron excess energy relative to the Fermi level, is controlled experimentally by the strength of the electrical current. As mentioned above, we expect the main contribution on L_Φ to be due to electron-electron scattering. A detailed theoretical treatment of the temperature-dependent Coulomb inelastic broadening in the pure two-dimensional case was given by Giuliani and Quinn.¹⁹ They found, including only the momentum-conserving electron-electron scattering processes, for $T \neq 0$ and $\Delta \ll k_B T \ll E_F$,

$$\frac{1}{\tau_{ee}} \Big|_{e-h} \simeq -\frac{E_F}{2\pi\hbar} \left[\frac{k_B T}{E_F} \right]^2 \times \left\{ \ln \left[\frac{k_B T}{E_F} \right] - 1 - \ln \left[\frac{2q_{\text{TF}}}{k_F} \right] \right\}, \quad (4)$$

and for $T = 0$ and $\Delta \ll E_F$,

$$\frac{1}{\tau_{ee}} \Big|_{e-h} \simeq -\frac{E_F}{4\pi\hbar} \left[\frac{\Delta}{E_F} \right]^2 \left\{ \ln \left[\frac{\Delta}{E_F} \right] - \frac{1}{2} - \ln \left[\frac{2q_{\text{TF}}}{k_F} \right] \right\}. \quad (5)$$

q_{TF} is the Thomas-Fermi screening wave vector and k_F the Fermi wave vector in the two-dimensional electron gas. In the experiment, however, we have a whole distribution of electron excess energies with a maximum value, called $\tilde{\Delta}$, which is proportional to the value Δ in Eq. (5). Increasing the temperature or the current implies an increase of the surplus electron energy above E_F and hence, an increased electron-electron scattering rate.

Figures 4 and 5 show two series of measurements, the first demonstrating the influence of temperature and the

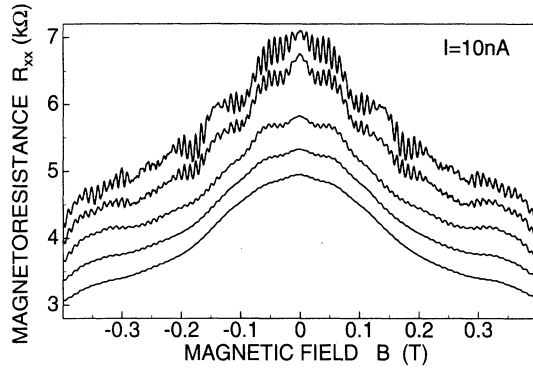


FIG. 4. Magnetoresistance R_{xx} versus magnetic field at $I = 10$ nA for a series of temperatures. From top to the bottom: $T = 0.33$ K, 2 K, 5 K, 7 K, 10 K. The curves are vertically offset for clarity by a value of 300 Ω .

second the dependence of the oscillations on the electron excess energy ($\tilde{\Delta}$). The strong Aharonov-Bohm oscillations observed with a current of 10 nA at 330 mK die out if either the temperature or the excess energy is enhanced. We have analyzed the amplitude of Aharonov-Bohm oscillations in the field range of $-0.4T < B < 0.4T$ using Eq. (2).

The phase coherence lengths L_Φ deduced from the T and $\tilde{\Delta}$ dependent data are presented in Fig. 6. Obviously, L_Φ saturates at low temperatures and the saturation value decreases with increasing $\tilde{\Delta}$. In accordance with the expected two-dimensional behavior,²⁰ the saturation occurs at higher temperatures if the electron excess energy increases. As long as $\tilde{\Delta}$ is smaller than $k_B T$, the thermal smearing of the Fermi edge, L_Φ is approximately identical for all electron excitations. For $\tilde{\Delta} > k_B T$, the temperature-independent effect becomes dominant and the saturation levels for different values of $\tilde{\Delta}$ become observable.

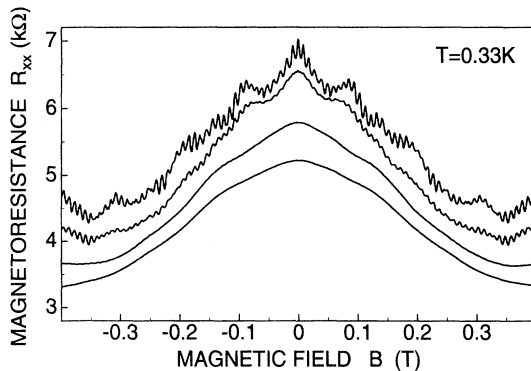


FIG. 5. Magnetoresistance R_{xx} versus magnetic field at $T = 0.33$ K for a series of electron excess energies $\tilde{\Delta}$. From top to the bottom: $\tilde{\Delta} = 0.054$ meV, 0.8 meV, 3.25 meV, 6.2 meV. The curves are vertically offset for clarity by a value of 300 Ω .

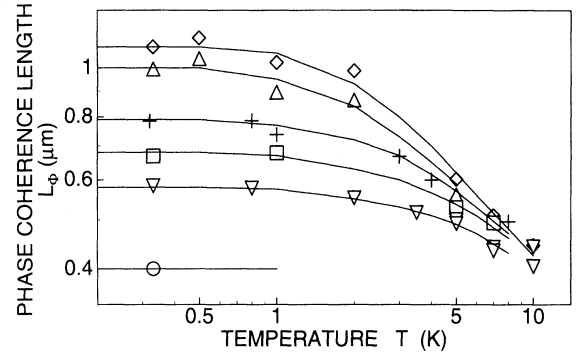


FIG. 6. Calculated phase coherence length L_Φ as a function of temperature for various electron excess energies [$(\diamond) \tilde{\Delta} = 0.054$ meV, $(\triangle) \tilde{\Delta} = 0.27$ meV, $(+)$ $\tilde{\Delta} = 0.56$ meV, (\square) $\tilde{\Delta} = 0.8$ meV, (∇) $\tilde{\Delta} = 1$ meV, (\circ) $\tilde{\Delta} = 3.25$ meV] ($E_F \approx 38$ meV). Lines are plotted as guidance to the eyes.

However, it turns out that there is a maximum in the saturation value for L_Φ of around 1.1 μm , which is reached for $\tilde{\Delta} = 0.1$ meV. Reducing $\tilde{\Delta}$ further to 0.01 meV leads to the same saturation value. Hence, there must be additional mechanisms limiting the phase coherence length L_Φ which is independent of temperature and current. We consider two possible mechanisms: spin-orbit scattering and broadening of the electronic states at the Fermi level due to elastic scattering by alloy induced disorder and/or by ionized impurities. Remember that the 2DEG in the present heterostructure is located in the ternary compound $\text{In}_x\text{Ga}_{1-x}\text{As}$. Spin-orbit scattering, which would manifest itself in antilocalization and should lead to a positive magnetoresistance,²¹ was not observed in the temperature range investigated here [see Fig. 2(a)]. Although we cannot exclude other effects, we can explain the observed saturation of L_Φ by ionized impurities. Ionized impurity scattering broadens the electronic states at the Fermi level by $\delta E \approx \hbar/\tau_{el}$. Thus, the phase space for scattering is no longer reduced for temperatures T below $\delta E/k_B$ and L_Φ is limited to a value of around 1.1 μm . With $\mu \approx 37$ m^2/Vs , we calculate a critical value for T of about 1 K in accordance with the observed bending of the curve in Fig. 6 for $\tilde{\Delta} = 0.054$ meV.

As mentioned before, Fasol⁴ has predicted, for the one-dimensional case and in the temperature range considered here, no dependence of L_Φ on Δ . Figure 6 shows that obviously the pure one-dimensional transport regime is not yet realized in our samples. The value of $W \approx 85$ nm for the rings exceeds π/k_F and, thus, we are dealing with more than one one-dimensional conducting channel. Additional information about the sample dimensions can be obtained by analyzing the slope of $L_\Phi(T)$ in the range where $k_B T > \tilde{\Delta}$. We find the phase coherence length to be proportional to T^{-p} with $p = 0.53$. Comparison with Eq. (4) yields a discrepancy between experiment and theory, where a value of p between 2 in the ballistic transport regime and 1 for diffusing electrons is expected. Including momentum-nonconserving

electron-electron scattering events, Al'tshuler *et al.*²² have calculated τ_Φ in disordered metals for one, two, and three dimensions. In the presence of ionized impurities or fluctuations in the boundary potential, the expected exponent $-p$ of the temperature becomes $1/4 < p < 2/3$ for electron transport in one dimension and $1/2 < p < 1$ in the two-dimensional case. Comparison with our experimental data gives two major results. First, the dimensionality of the electron transport in our rings is between one and two. Second, there is a remarkable effect of momentum-nonconserving scattering processes in our samples.

Finally, we discuss the advantages of $\text{In}_x\text{Ga}_{1-x}\text{As}/\text{InP}$ heterostructures for electron interference devices. The dependence of the phase coherence length on the carrier concentration n_s and on the carrier mass m^* is given in the diffusive and in the ballistic regime by^{5,20,23}

$$L_\Phi = \sqrt{D} \tau_\Phi \sim \frac{n_s \sqrt{\mu}}{m^*} \quad \text{diffusive regime} \quad (6)$$

$$L_\Phi = v_F \tau_\Phi \sim \frac{n_s^{3/2}}{m^{*2}} \quad \text{ballistic regime.} \quad (7)$$

Here, it is assumed, that electron-electron scattering is the process limiting the phase coherence length. Then, according to Eqs. (4) and (5), τ_Φ is proportional to E_F , i.e., $\tau_\Phi \sim n_s/m^*$. The diffusion coefficient $D = v_F^2 \tau_{el}/2 = \pi \hbar^2/e \times n_s \mu/m^*$ is expressed in terms of the mobility μ , the Fermi velocity v_F is given by $\hbar \sqrt{2\pi n_s}/m^*$. Obviously the effective mass m^* plays a crucial role for the absolute value of L_Φ . In our strained $\text{In}_x\text{Ga}_{1-x}\text{As}/\text{InP}$ system, we have determined m^* by the temperature dependence of Shubnikov-de Haas oscillations and have found $m^* = 0.037m_0$.¹⁸ In comparison, the effective electron mass in an $\text{Al}_x\text{Ga}_{1-x}\text{As}/\text{GaAs}$ heterostructure is $m^* = 0.067m_0$. Beside this, n_s values of approximately $6.5 \times 10^{11} \text{ cm}^{-2}$ with only one populated two-dimensional subband and no bypass in the doped layer cannot be reached in the $\text{Al}_x\text{Ga}_{1-x}\text{As}/\text{GaAs}$ system, where the sheet carrier concentration in typi-

cal layer systems is limited at around $4.5 \times 10^{11} \text{ cm}^{-2}$. Mainly DX centers are responsible for the Fermi level pinning over a wide range of various dopant concentrations, thus preventing high electron concentrations in the two-dimensional channel. Although higher values of electron mobility can be obtained in a 2DEG formed in GaAs, the influence on the phase coherence length is compensated by the effective mass and the sheet carrier concentration. The advantage of the $\text{In}_x\text{Ga}_{1-x}\text{As}/\text{InP}$ heterostructure becomes even more pronounced in the ballistic transport regime, where there is no influence of mobility on L_Φ but a large influence of concentration and effective mass. In addition, the system under investigation does not show any depletion zone at the edges of the rings. As a consequence, the lithographical structure is identical with the electrically active structure.

IV. CONCLUSIONS

In summary, we have fabricated mesoscopic rings in a strained high mobility $\text{In}_{0.77}\text{Ga}_{0.23}\text{As}/\text{InP}$ heterostructure, where periodic oscillations in the magnetoresistance due to Aharonov-Bohm effect can be observed. The major phase breaking mechanism below 10 K is electron-electron scattering. The dependence of L_Φ on temperature, electron excess energy $\tilde{\Delta}$, and on disorder related scattering are clearly established. The dimensionality of the transport in the ring is between one and two and there is evidence of nonconservation of electron momentum in electron-electron scattering in a disordered system. Finally, the small effective mass and the high electron concentration in the 2DEG in strained $\text{In}_{0.77}\text{Ga}_{0.23}\text{As}/\text{InP}$ heterostructures make this system an excellent candidate for devices based on interference phenomena.

ACKNOWLEDGMENT

The author would like to thank G. Müllejans for his help in the measurements.

¹ B. Laikhtman, U. Sivan, A. Yacoby, C. P. Umbach, M. Heiblum, J. A. Kash, and H. Shtrikman, *Phys. Rev. Lett.* **65**, 2181 (1990).

² F. Müller, B. Lengeler, Th. Schäpers, J. Appenzeller, A. Förster, Th. Klocke, and H. Lüth, *Phys. Rev. B* (to be published).

³ H. L. Störmer, L. N. Pfeiffer, K. W. Baldwin, and K. W. West, *Phys. Rev. B* **41**, 1278 (1990).

⁴ G. Fasol, *Appl. Phys. Lett.* **61**, 831 (1992).

⁵ K. Aihara, M. Yammamoto, K. Iwodate, and T. Mizutani, *Jpn. J. Appl. Phys.* **30**, L1627 (1991).

⁶ H. Hardtdegen, R. Meyer, H. Løken-Larsen, J. Appenzeller, Th. Schäpers, and H. Lüth, *J. Cryst. Growth* **116**, 521 (1992).

⁷ H. Hardtdegen, R. Meyer, M. Hollfelder, Th. Schäpers,

J. Appenzeller, H. Løken-Larsen, Th. Klocke, Ch. Dieker, B. Lengeler, and H. Lüth, *J. Appl. Phys.* **73**, 4489 (1993).

⁸ Th. Klocke, *Ber. Forschzent. Jüil.* **Jül-2723**, 1 (1993).

⁹ S. Washburn, R. A. Webb, and T. J. Watson, *Adv. Phys.* **35**, 375 (1986).

¹⁰ R. A. Webb, S. Washburn, C. P. Umbach, F. P. Milliken, R. B. Laibowitz, and A. D. Benoit, *Physica A* **140**, 175 (1986).

¹¹ F. P. Milliken, S. Washburn, C. P. Umbach, R. B. Laibowitz, and R. A. Webb, *Phys. Rev. B* **36**, 4465 (1987).

¹² G. Timp, A. M. Chang, P. De Vegvar, R. E. Howard, R. Behringer, J. E. Cunningham, and P. Mankiewich, *Surf. Sci.* **196**, 68 (1988).

¹³ H. van Houten, C. W. J. Beenakker, M. E. I. Broekaart, M. G. H. J. van Heijman, B. J. van Wees, H. E. Mooij, and

- J. P. Andre, *Acta Electron.* **28**, 27 (1988).
- ¹⁴ P. A. Lee and A. Douglas Stone, *Phys. Rev. Lett.* **55**, 1622 (1985).
- ¹⁵ J. A. Simmons and D. C. Tsui, *Surf. Sci.* **196**, 81 (1988).
- ¹⁶ S. Datta and S. Bandyopadhyay, *Phys. Rev. Lett.* **58**, 717 (1987).
- ¹⁷ A. Menschig, A. Forchel, B. Roos, R. Germann, K. Pressel, W. Heuring, and D. Grützmacher, *Appl. Phys. Lett.* **57**, 1757 (1990).
- ¹⁸ D. Uhlisch, Master's thesis, Rheinisch-Westfälische Technische Hochschule-Aachen, 1994.
- ¹⁹ G. F. Giuliani and J. J. Quinn, *Phys. Rev. B* **26**, 4421 (1982).
- ²⁰ G. Fasol, *Appl. Phys. Lett.* **59**, 2430 (1991).
- ²¹ Y. K. Fukai, S. Yamada, and H. Nakano, *Appl. Phys. Lett.* **56**, 2123 (1990).
- ²² B. L. Al'tshuler, A. G. Aronov, and D. E. Khmel'nitskii, *J. Phys. C* **15**, 7367 (1982).
- ²³ A. Yacoby, U. Sivan, C. P. Umbach, and J. M. Hong, *Phys. Rev. Lett.* **66**, 1938 (1991).

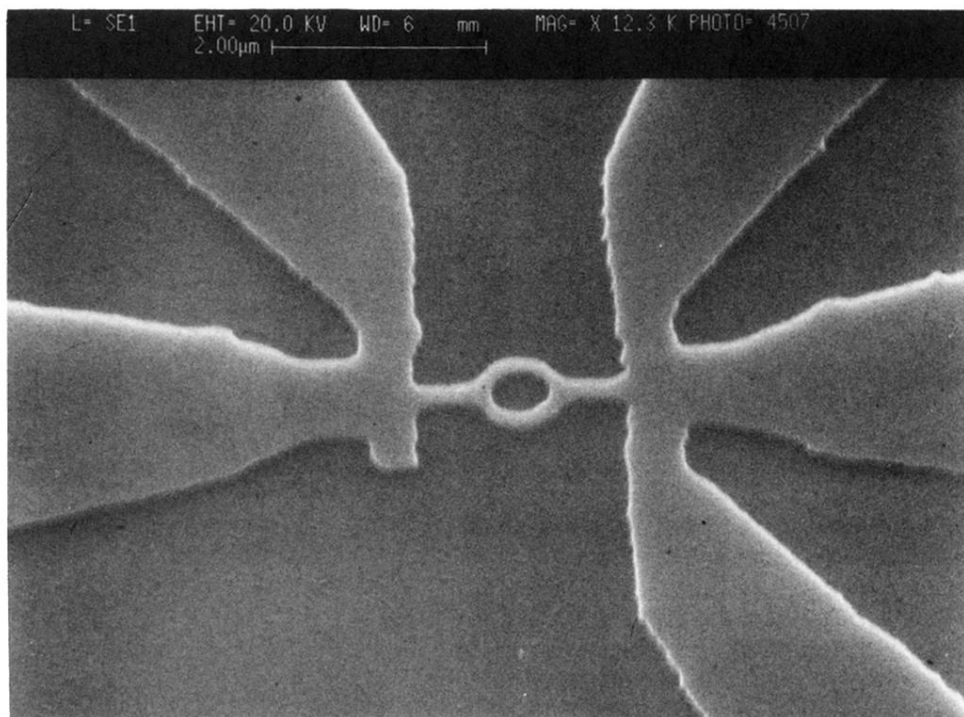


FIG. 1. Scanning electron micrograph of a typical ring under investigation.